Environmental Technology & Innovation 18 (2020) 100786

Contents lists available at ScienceDirect

Environmental Technology & Innovation

journal homepage: www.elsevier.com/locate/eti

Novel cellulose nanofiber aerogel for aquaculture wastewater treatment

Fatemeh Darabitabar [a], Vahid Yavari [a], Aliakbar Hedayati [b,*], Mohammad Zakeri [a], Hossein Yousefi [c]

[a] Faculty of Marine Natural Resources, Khorramshahr University of Marine Science and Technology, Khorramshahr, Iran
[b] Faculty of Fisheries and Environmental Sciences, Gorgan University of Agricultural Sciences and Natural Resources, Gorgan, Iran
[c] Laboratory of Sustainable Nanomaterials, Department of Wood Engineering and Technology, Gorgan University of Agricultural Sciences and Natural Resources, Gorgan, Iran

ARTICLE INFO

Article history:
Received 11 February 2020
Received in revised form 1 April 2020
Accepted 1 April 2020
Available online 8 April 2020

Keywords:
Nano adsorbent
Environmental remediation
Polysaccharide
Wastewater treatment

ABSTRACT

A cellulose aerogel containing safe and environmentally-friendly crosslinkers (carboxy methyl cellulose/citric acid) was used to purify aquaculture wastewater through removing nitrate, nitrite, and phosphate compounds. The results showed that the produced aerogel has a specific surface area of 300 m/g, the density of 0.004 g/cm^3 and porosity of 99.68%. The optimum adsorbent were calculated at a constant weight of 0.1 g, pH = 6, time 60 min, concentration 100 mg/l, and temperature 30 °C. The adsorption isotherm models showed the most agreement with the Temkin and the Langmuir models and the second pseudo order, confirming the high capability of aerogel in physical and chemical adsorption. The highest removal efficiency of nitrate, nitrite, and phosphate obtained were 79.65, 73.04, and 98.18%, respectively. Cellulose nanofiber aerogel without additional coating and harmful chemical compounds could be used as an effective adsorbent in wastewater treatment.

1. Introduction

Agricultural wastes with high amounts of cellulose can remove various types of contaminants. Cellulose is a biopolymer used in laboratory, pilot and industrial scales without toxic waste (Yousefi et al., 2015). Today, the use of different approaches such as chemical, physical and biological methods are employed to remove the various contaminants. But, each of these methods has disadvantages, such as the use of toxic compounds, the high cost of production and maintenance, the enjoyment of specific requirements for the maintenance of biological species and the non-biodegradability, and so on (Rafieian et al., 2018). The use of nano-adsorbents to remove environmental pollutants has attracted the attention of many researchers (De France et al., 2017). Plant-derived nano-adsorbents, like nanocellulose, can be an effective and efficient materials for the removal of pollutants from water/wastewater without harmful compounds (Zheng et al., 2014). With the enjoyment of unique features, such as high specific strength, renewability, availability and cheapness, the high aspect ratio leading to the creation of a solid and networked structure, high specific surface area and relatively low density cellulose nanofibers (CNF), which can be used as a suitable option for the fabrication of useful nano-adsorbents (Long et al., 2018; Yousefi et al., 2018). The use of these nanostructures in the production of CNF aerogels generates valuable products for the protection and sustainability of environment and adherence to green chemistry principles and rules

* Corresponding author.
E-mail address: Hedayati@gau.ac.ir (A. Hedayati).

https://doi.org/10.1016/j.eti.2020.100786
2352-1864/

(Sehaqui et al., 2011) and can resolve a lot of environmental problems in different areas, especially the fisheries industry that requires high water consumption. The waste water of fish farms contains a large amount of nitrogen and phosphate compounds. With the introduction of these compounds into the body of aquatic ecosystems, especially rivers, it results in increased organic load and the occurrence of eutrophication phenomena, leading to algae blooms and deaths of many aquatics. Moreover, returned wastewater treatment and its reuse will compensate many costs of production and shortage of fresh water and will remarkably reduce final consumption costs (Jana et al., 2018).

Aerogels are materials that consist of 95%–99% of the air, which has a high surface area and very low density (De France et al., 2017). CNF aerogels are materials with porous structure, very low density and high specific surface area that are produced under supercritical and freeze-drying conditions (Gopakumar et al., 2019). These aerogels are used in various applications, such as acoustic thermal insulations, super-absorbents and batteries because of having features such as high strength and resistance, cheaper production compared to other aerogels and environmentally friendly properties and biodegradability (Shamskar et al., 2019). Citric acid (CA) is among the natural organic acids in some fruits such as oranges and lemons. This acid is non-toxic and inexpensive and is used in many food and drug industries and is approved by FDA (Demitri et al., 2008). Citric acid with one hydroxyl group and three carboxyl groups is considered as the main organic acid in the creation of cross-links (Reddy and Yang, 2010). Carboxylic acid groups can form strong hydrogen bonds with cellulose nanofibril hydroxyl groups. The substance is nutritionally safe and metabolites thereof is harmless to humans (Shi et al., 2007).

In a study conducted by Kaya in 2017 to create cross-links in the structure of cellulose with citric acid, the results confirmed the establishment of a strong cross-link between citric acid and cellulose structure and increasing the capability of aerogels (Kaya, 2017). Carboxymethyl cellulose (CMC) is a natural polymer soluble in water made of cellulose and has the stabilizing, thickening, non-toxic and safe properties (Zheng et al., 2015) and has antimicrobial properties (Dashipour et al., 2014) and is used in various industries including pharmaceutical and food industries instead of natural materials that are expensive (Ogushi et al., 2007). One of the problems in the manufacture of CNF aerogels for use in the fields of water and wastewater treatment is the use of acrylamide and acrylic acid compounds to form cross-links or tight cross-links in order to prevent breakdown of cellulosic structure after the adsorption of water. The use of acrylamide and acrylic acid compounds can be highly toxic and dangerous to human health and other organisms (LoPachin, 2004). In the current study, we tried to eliminate this problem through replacing a safe and biodegradable CNF aerogel containing crosslinker components (CMC/CA) approved by the FDA organization. The combination of citric acid with CMC in the structure of CNFs can form a very strong cross-linking and causes a creation of superabsorbents with a lot of capabilities.

In addition to creating a strong polymeric network and maintaining the aerogel structure in water, crosslinking in aerogel structures could absorbs water because of carboxymethyl cellulose and nano fiber cellulose in the aerogel structure. The presence of physical and chemical bands in the nano-cellulose aerogel structure increases the rate and efficiency of adsorption. Binding of aldehyde functional groups at the cellulose structure surface to the carboxylic acid groups of citric acid and sodium carboxy-methyl cellulose causes strong bonding and bonding. This could absorbs ions and ion exchanges with the groups participating in the reaction. Creating electrostatic force in acidic medium increases the adsorption on adsorbent surfaces. This also increases the protonation of the adsorbent surfaces and increases the tension between the adsorbent and adsorbant and increases the uptake of nitrate, nitrite and phosphate ions. So this study focuses on the production of new safe cellulose nanofiber superabsorbent bearing high water adsorption capacity, specific surface area and mechanical strength to remove nitrogen and phosphate compounds from waste water of warm water fish culture farms.

2. Materials and methods

2.1. CNF production

CNF was prepared from alpha cellulose of bagasse (sugarcane wastes) by a super disk grinder (MKCA6-2; Masuko Co., Japan) in Nano Novin Polymer Co. (Iran). The production of highly pure alpha-cellulose fibers from bagasse was described elsewhere. Briefly, 1 wt% cellulose fiber water slurry was passed three times through with the grinder at 1500 rpm to prepare CNF.

2.2. CNF aerogel production

First, 80 wt % of the CNF suspension put on the shaker at 80 °C at 100 rpm. Then, carboxy methyl cellulose (CMC;Sigma-Aldrich Co.) and citric acid (CA; Merk Co.), each 10 wt%, were dissolved in 10 ml of distilled water. The CNF suspension was then added to the solution of CMC/CA and stirred at 70 °C for 30 min to obtain highly viscose CNF-based gel. Finally, the highly viscose gel was frozen in liquid nitrogen followed by drying in a freeze dryer (Beta 2-8 LD Plus; Christ Co., Germany) for 72 h at −50 °C, resulted in CNF aerogel, also hydrochloric acid was used for 30 min to protonate the bands.

2.3. Determination of experimental conditions for wastewater purification

To determine the optimum adsorption conditions, the experiment was performed in a batch system so that one of the parameters was considered constant at each stage. The selected parameters were selected based on the minimum and maximum adsorption rates. The parameters including adsorbent weight were selected as constant 0.1 g, pH (4–8), contact time (0–90) min and waste water concentration (25–100) mg per liter. The process of test was in a way that appropriate pH with optimum adsorption efficiency was initially selected. Then, all experiments were carried out at the pH obtained. Next, concentration, contact time and optimum temperature were determined. First, 100 ml of wastewater with a desired concentration was poured into 200 ml Erlenmeyer flask. After that, by controlling pH of the solution, a certain amount of adsorbent (CNF aerogel) was added to the solution, and the Erlenmeyer flask was subjected to stirring at 150 rpm at ambient temperature on a hot plate for a certain time. This stage was carried out to provide a better contact of nano-adsorbent with wastewater (Askari Hesni et al., 2020).

2.4. Characterization of CNF aerogel

To examine the morphological and internal structure of the aerogels as well as the porosity types, field emission scanning electron microscope (FE-SEM) was used. To carry out this test, the specimens were initially coated with a thin gold nanoparticles, and imaging was performed using a FE-SEM (MIRA3TESCAN-XMU , Czech Republic). The energy dispersive spectroscope (EDS) test was used to identify the constituent elements and determine their percentages in the aerogel. Atomic force micrographs of CNF were prepared using an atomic force microscope (AFM; SII Nanotechnology, Inc., Japan) equipped with Si probe.

Fourier-transform infrared spectroscopy (FTIR) was carried out to determine the functional groups available in the structure of the aerogel within wavelength range (400–4000 cm^{-1}) using FTIR model Tensor II manufactured by Bruker Co. Germany. X-ray diffraction (XRD) test was performed to determine the crystal structure of the aerogels within the angle of $2\theta = 5°–50°$ and temperature 25 °C by XRD model PW1730, Netherlands. Crystallinity index (CrI) was evaluated using the following Eq. (1):

$$\mathrm{CrI} = 100(\mathrm{I} - \mathrm{I}_{\beta})/\mathrm{I} \tag{1}$$

where I is the diffraction intensity assigned to the 200 reflection of cellulose I_β, which is typically in the range $2\theta = 21°–23°$. I_β is the intensity measured at $2\theta = 18°$, where the maximum occurs in a diffractogram for non-crystalline cellulose. Thermogravimetric analysis (TGA) test was conducted in the temperature range of 0–600 °C at a temperature rate of 10 °C/min with the TG 209F3 NETZSCH manufactured in Germany. To determine the amount of porosity, pore size and specific surface area, BET test was performed with BET device, model BELSORP MINI II made in Japan using nitrogen gas at a temperature of −196 °C.

2.5. Adsorption models

To measure the adsorption rate, a photometer machine (Model 7100, Wagtech Co., UK) was used. In order to measure the optimum value and calculate the removal rate and evaluate the isotherm, kinetic and thermodynamic tests, the calculations of Table 1 were used. To calculate the removal rate, Eq. (2) was used. In this equation, C0 and Ce are respectively the initial concentration and final concentration in milligrams per liter. In order to evaluate the amount of adsorption capacity, Eq. (3) was used. In this equation, qe is the equilibrium adsorption capacity in milligrams per gram, C0 initial concentration in milligrams per liter, Ce final concentration in milligrams per liter, V volume of solution in liters and m adsorbent weight in grams. In order to calculate adsorption models from the Langmuir model, it is assumed that the adsorption process takes place at similar sites with the same energy distribution and the adsorption is monolayer Eq. (4). In this model, q_m (mg/l^{-1}) is the maximum adsorption rate and K_L (l/mg^{-1}) is the Langmuir constant coefficient, which are both dependent on adsorption capacity and energy Eq. (5) (Tajari et al., 2019). In this equation, Kf and n are the Freundlich model constants that indicate the adsorption capacity and intensity, respectively. In the Temkin isotherm model, it is assumed that the adsorption heat of all the molecules on the adsorbent surface is linearly reduced. In this model, KT and BT are constants of this model and b is a constant that depends on the heat of adsorption (Eq. (6), Table 1). Thermodynamic studies reflect the spontaneous of processes, the exothermic and endothermic reactions, and the enthalpy and entropy changes of adsorption (Eqs. (7) and (8)). In this equation, $\Delta G°$ Gibbs free energy, $\Delta S°$ entropy and $\Delta H°$ enthalpy, R the universal gas constant in kJ/mol, T temperature in Kelvin and b the process equilibrium constant (Ebrahimi et al., 2019; Safaei et al., 2019). To calculate the water adsorption, first, the sample put in water at room temperature for 20 min until it was completely saturated, followed by weighing with a digital scale to obtain its saturation weight (W_1; Eq. (12), Table 1). The saturated sample was then dried completely in an oven overnight followed by weighing its dry weight W_2; Dry weight, Eq. (12), Table 1).

2.6. Desorption

To desorption experiment, NaOH was added to adsorption optimizations at 120 rpm. To investigate the rate of desorption a desorption equation was used (Table 1, (11)). In this equation, C_e (mg/l) is the concentration of unabsorbed pollutant, and C_0 (mg/l) is the initial concentration of the pollutant and C_R (mg/l) is the pollutant concentration in the wash solution during the adsorption process.

Table 1
Adsorption models used in this study.

Removal rate % (2)	$R = \frac{C_0 - C_e}{C_0} \times 100$
Adsorption capacity (3)	$q_e = \frac{(C_0 - C_e)V}{m}$
Langmuir (4)	$\frac{C_e}{q_e} = \frac{1}{qm} + \frac{1}{KLqm}$
Freundlich (5)	$Lnq_e = LnK_f + \frac{1}{n} LnC_e$
Temkin (6)	qe = B_T ln K_T + B_T ln C_e
Pseudo first-order (7)	log($q_e - q_t$) = logqe − K1/2/303 t
Pseudo second-order (8)	$\frac{t}{qt} = \frac{1}{K_2 q_e^2} + \frac{1}{q_e} t$
Gibbs free energy equation (9)	$\Delta G^0 = \Delta H^0 - T\Delta S^0$
Van't hoff equation (10)	$\ln K_c = \frac{\Delta S^0}{R} - \frac{\Delta H^0}{RT}$
Desorption % (11)	$R = \frac{C_R}{C_0 - C_e} \times 100$
Water adsorption % (12)	$R = \frac{W_1 - W_2}{W_2} \times 100$

3. Results and discussions

Fig. 1 shows AFM micrograph of CNF and FE-SEM micrograph of CNF aerogel produced in this study. CNFs had an diameter ranged from 22 to 54 nm (averagely 35 ± 10 nm) and a high length to diameter ratio. CNF aerogel showed a very porous structure. The BET test indicated a specific surface area of 300 m^2/g, density of 0.004 g/cm^3 and a porosity of 99.68% for CNF aerogel. The amount of water adsorption by the aerogel was also measured to be 3328.57%. This high amount of water absoption is attributed to the high specific surface area and high amount of available OH groups as well as highly networked structure of CNF aerogel provided high capillary force to absorb water (Yousefi et al., 2018).

Fig. 1 also shows digital photos of very light weight CNF aerogel. The connection of carboxylic groups of CA to CMC groups makes hydrogen bonds between the polymer chains and creates strong crosslinks between CMC with CNF aerogel. Carboxylic acid can be easily dissolved in water, but its solubility decreases with increasing the length of carbon chain which occurs in reaction. This structure helps aerogel to maintain its internal structure. The carboxylic (C (= O) OH) citric acid groups attached to the bottom of the CMC chain in the cellulose nanofibers create a strong cross-link between the CMC polymer chains.

Fig. 2-a depicts TGA trace of CNF aerogel. The weight loss of aerogel up to 150 °C was related to loss of moisture. Thermal analysis curve represents two stages of high weight loss of aerogel at onset temperatures of around 150 °C and 290 °C. First significant weight loss was generated because of citric acid thermal degradation. The second step of aerogel weight loss belongs to the combination of CMC and CNF, which occurred at a temperature of around 290 ° C, representing the thermal stability of CNF and CMC is greater than that of citric acid. In the final step, about 27% of ash remained from the tested aerogel.

Fig. 2-b depicts the XRD patterns of CNF aerogel before and after absorption. The XRD pattern of aerogel before absoption showed peaks at 2θ of 15, 16, 22.5 and 35.5 degrees, which are typically for cellulose I_β. Among these four peaks the peak appeared at 2θ of 22.5 degree was the strongest one, assigned to the atomic plane of [200] of cellulose I_β crystallite. These results confirmed that the main structure of the aerogel is made of cellulose I_β, demonstrating that CMC and CA were both dissolved within fabrication process and participated in crosslinkages; hence, no trances of their crystallites could be seen in the XRD profiles. After absoption the XRD pattern of aerogel showed peak broadening. The CrI of aerogel before and after absorption obtained were 70% and 38%. According to the data, it could resulted the absorbed components had mainly amorphous structure; hence, the amorphous portion of aerogel increased, resulted in peak broadening and a drastic reduction of CrI.

Fig. 2-c shows FTIR curves of CNF aerogel before and after absorption. According to the form of FTIR test, The peak of 2896.65 cm^{-1} is related to a strong bond of alkyl functional groups and aliphatic compounds. It also indicates the H–C strong bond. The peaks 1158.09–1029.94 cm^{-1} can be related to the C–O strong band at the ether structure in CNF aerogel (Ciolacu et al., 2011; Haafiz et al., 2013). The bond 3338.71 cm^{-1} can be attributed to the acid and methanol functional groups and the strong bond 1063.98 cm^{-1} is related to the $C - O - C$ functional group (Fan et al., 2012). The peak 1714.53 cm^{-1} can be related to carbonyl strong bond at the citric acid group to react with a hydroxyl group in the CNF (Coma et al., 2003; Demitri et al., 2008). The peak of 1030.57 cm^{-1} can be attributed to the ether and pyranose functional group. The strong bond of 1370.46 cm^{-1} is related to the CH2, CH3, OH, and C–O functional groups and the bond 894.53 can be considered as the representation of the amorphous region in the nano-cellulose (Morán et al., 2008; Reddy and Yang, 2005). The peaks observed changes in before and after the adsorption indicates the involvement of C–O–C, C–O, carbonyl and carboxylic acid functional groups in the aerogel structure.

Fig. 3-a shows the effect of pH on the absoption of nitrate, nitrite and phosphate compounds by CNF aerogel at the time of 60 min, adsorbent weight of 0.1 g and concentration of 100 ppm. By changing the pH from 4 to 6, the adsorption efficiency increased and the adsorption rate on nitrate, nitrite and phosphate compounds were measured to be 79.14%, 75.65% and 99.09%, respectively. By increasing the pH, the removal rate in nitrate, nitrite and phosphate compounds

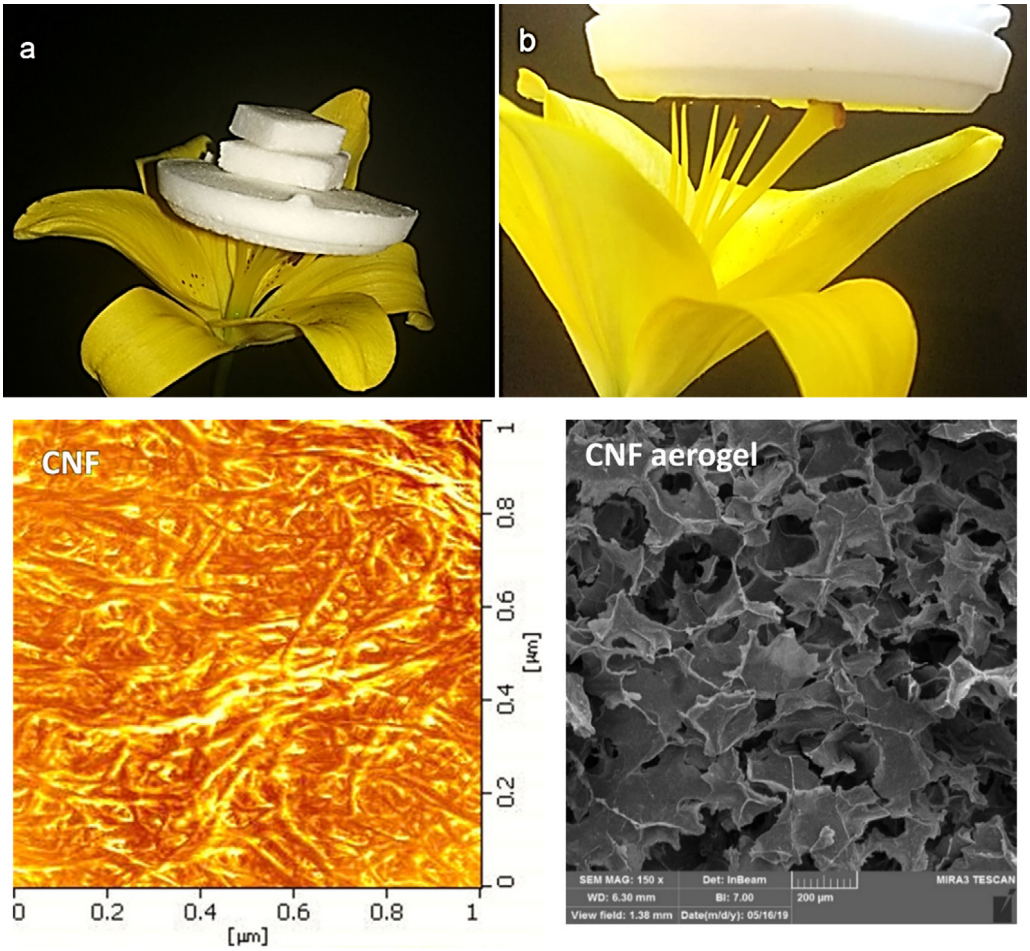

Fig. 1. CNF aerogel produced in this study (a,b); AFM micrograph of CNF and FE-SEM micrograph of CNF aerogel.

was calculated to be 43.07%, 12.17% and 49.09%, respectively. This is because with the increase of hydroxyl groups in solution and competition with adsorbed ions for binding to active adsorption sites at the adsorbent surface, the adsorption efficiency decreased. Indeed, acidic environments increased H+ at the active adsorption sites on the adsorbent and increase the removal rate. The pH determines the electron charge of the adsorbent surface, the separation of the functional groups at the active adsorption sites, and the ionization rate of the substances in the solution. As can be seen in Fig. 3, the adsorption performance and efficiency increased in the range of acidic pH. In the acidic pH, the active adsorption sites of carbonyl and carboxylic groups present in the structure of nano-adsorbent were protonated and the positive electron charge density on the surface and the internal structure of the adsorbent rised. So, the adsorption efficiency of anionic compounds in the waste water increased because of the presence of electrostatic attraction. In the other mode, the nano-adsorbents with chloride ions to maintain the balance may be charged in acidic environments such as HCl. As a result, the anionic ions available in the solution were replaced with nano-adsorbent chloride in the ion exchange process. In the higher pHs, due to elevated of the negative charge density on the adsorbent area and the creation of electrostatic repulsive force between the negative electric charge of the adsorbent, the removal efficiency reduced (Fig. 3-a). PH is one of the important parameters that affects the adsorption rate and the ionization by changing the surface ionic charge and controls the adsorption process (Langeroodi, 2017). The amount of H+ ion at the acidic pH increases and the adsorbent surface is positively charged by adsorption of this ion. At the pHs 5 and 6, the removal rates reaches 78.63, 78.26 and 97.27 (at pH 5) and 79.14, 75.65 and 99.09 (at pH 6) for nitrate, nitrite and phosphate, respectively. In this study, pH 6 was selected as the optimal pH (Fig. 3). At the high pH, the proton attached to the hydroxyl functional groups in the adsorbent structure is isolated and weak interaction is formed between the contaminant and the adsorbent surface, which reduces the adsorption capacity.

Fig. 3-b depicts the effect of initial concentration on the adsorbent weight of 0.1 g, 60 min time and pH 6 on the adsorption rate of nitrogen and phosphate compounds. With increasing concentrations from 25 to 100 mg/l, the removal rate increased up to 98.18%, 76.52% and 78.29% for phosphate, nitrite and nitrate, respectively. This increase in adsorption

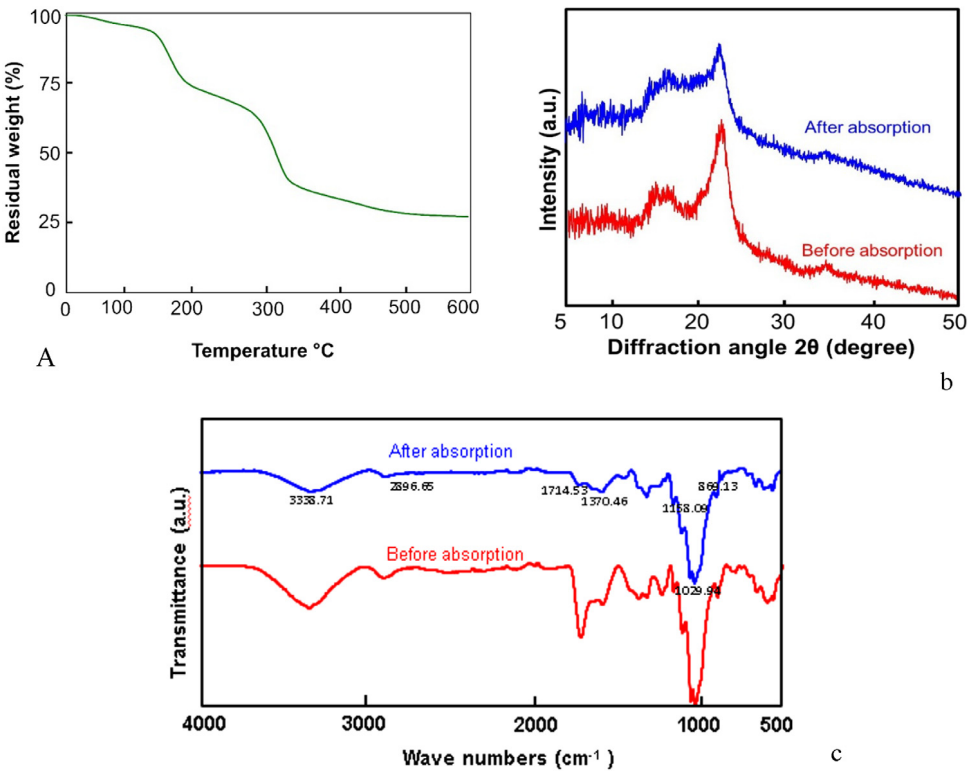

Fig. 2. Different characteristics feature of CNF aerogel. (a) TGA trace of CNF aerogel; (b) XRD patterns of CNF aerogel before and after absorption; (c) FTIR curves of CNF aerogel before and after absorption.

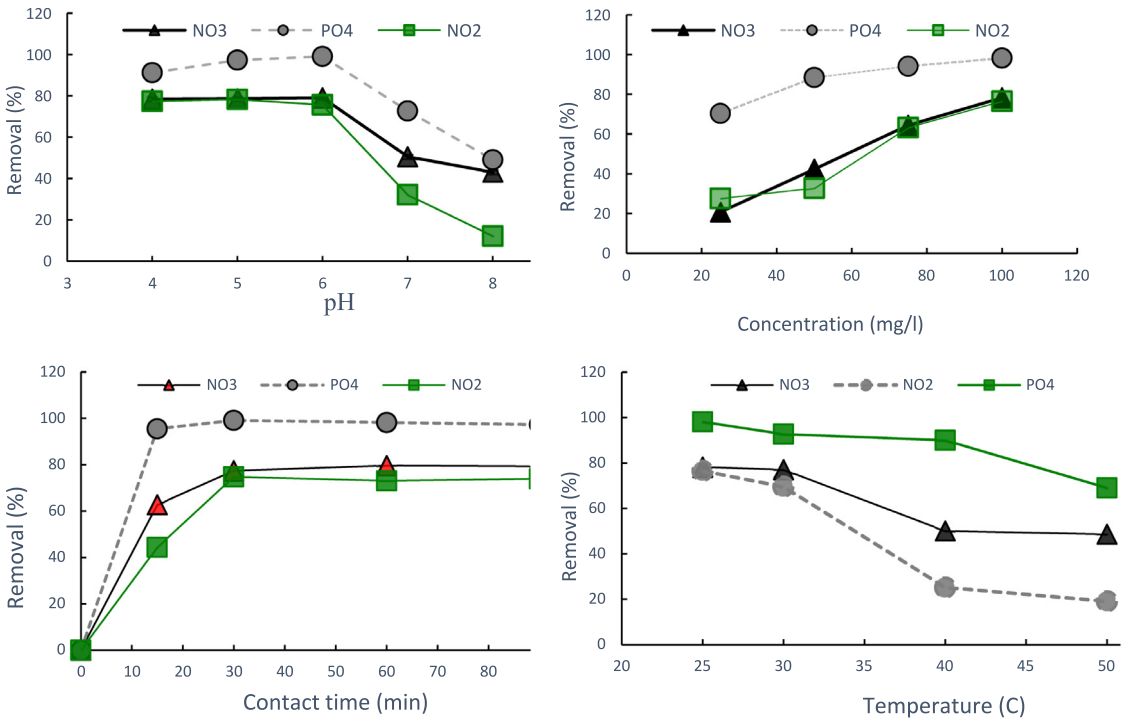

Fig. 3. The effect of different physiochemical parameters on the absoption of nitrate, nitrite and phosphate compounds by CNF aerogel. (a) pH (time = 30 min, concentration = 100 mg/l, weight = 0.1 g); (b) concentration (time = 30 min, pH = 6, weight = 0.1 g); (c) contact time (pH = 6, concentration = 100 mg/l, weight = 0.1 g); (d) temperature (time = 60 min, concentration = 100 mg/l, weight = 0.1 g, pH = 6).

can be due to the increased interaction of phosphate, nitrite and nitrate ions with the adsorption sites on the adsorbent surface. The reason for the high removal efficiency at high concentrations can be attributed to the proper propulsion in the solution, which leads to increasing the adsorption rate. At low concentrations, the contaminant was absorbed at the specific sites. These specific sites were saturated by increasing the concentration of contaminant. Because of this further contaminant was absorbed at exchange sites. Also, with increasing concentration, both removal rate and adsorbent capacity increased. The removal rate at the concentration of 100 mg/l was 78.29, 76.52 and 98.18 for nitrate, nitrite and phosphate respectively. In a study conducted by Wei et al. in 2019 on the fabrication of nano-cellulose-based magnetic hybrid aerogels, the results indicated that the magnetized aerogel with nano Fe_3O_4 were able to remove heavy metals such as chromium with a maximum removal rate of 2.2 mg per gram, representing the high capability of nano-cellulose aerogels in the field of water and wastewater treatment (Wei et al., 2019). The results of the current study demonstrated that the increase of removal rate with increasing concentration could be due to the increase in thrust force. In the research carried out by Azadbakht et al. (2016), the amount of optimum concentration to remove the nitrate with a cellulose nanocrystalline adsorbent was selected to be equal to 100 mg/L with a maximum removal of 8.33 mg/g (Azadbakht et al., 2016).

Fig. 3-c represents the effect of contact time (pH = 6, concentration = 100 mg/l, weight = 0.1 g) on the absoption of nitrate, nitrite and phosphate compounds by CNF aerogel. Contact time is an important parameter for accessing anionic compounds to the active functional groups at the nano-adsorbent surface, which is considered in the ranges of 15 to 90 min at a dose of 100 mg/L, pH 6, weight 0.1 g for the adsorption test. In the early times, the adsorption rate elevated rapidly because of the vacancy of adsorption sites at the adsorbent surface and the increased probability of the collision of ions with the adsorbent surface. At the time of 15 to 30 min, the adsorption rates of 77.43%, 74.78% and 99.09% were calculated for nitrate, nitrite and phosphate, respectively. The corresponding absorption values for the time of 60 min, were 79.65%, 73.04% and 98.18%, respectively. After this time, due to filling the active adsorption sites, the adsorption rate reached the equilibrium state. Investigation of the effect of contact time shows an increase in the removal rate from 15 to 30 min due to the vacancy of active sites in the adsorbent surface. With increasing the contact time, due to filling the adsorption sites and reducing the vacant positions on the adsorbent surface, the adsorption rate decreases and the adsorption reaches the equilibrium time. By increasing the contact time, the possibility of more contact of contaminant with the functional groups on the adsorbent surface increases, and the adsorption capacity and efficiency rise. In this regard, the optimum time of 60 min is selected. In a study performed by Tian et al. (2018), the performance of nano-cellulose aerogels in the removal of heavy metals was examined. In order to make crosslinks, acrylic acid was used. The maximum adsorption rate for copper and lead ions was measured to be 40.01 and 130.36 mg/g, respectively. The adsorption models that represented the most agreement in the aforementioned study were the isotherm model and the pseudo-second-order kinetics model. Chemical adsorption coupled with the physical adsorption composition were features of this produced aerogel (Tian et al., 2018). In the present study, the conformity with the Langmuir, Freundlich and Temkin second-order kinetics adsorption models confirmed the chemical and physical adsorption capacity of CNF aerogel, indicating its high capability and the existence of different types of structures in it.

Fig. 3-d depicts the effect of temperature (time = 60 min, concentration = 100 mg/l, weight = 0.1 g, pH = 6) on the absoption of nitrate, nitrite and phosphate compounds by CNF aerogel. At the initial temperatures, the adsorption rate increased. At the temperature of 30 °C, the adsorption rate in nitrate, nitrite and phosphate compounds was measured to be 77.09, 69.56 and 92.72, respectively. At the higher temperatures, the removal efficiency reduced, implying that the adsorption can be physical type at a lower temperature (Safaei et al., 2019). By elevating temperature from 30 °C to 50 °C, the removal rate and adsorption capacity decreased and reached 48.71, 19.13 and 69.09 in nitrate, nitrite and phosphate, respectively, representing the exothermic reaction. The negativity of ΔH° and ΔS° reflects the exothermic and physical process of adsorption and reduction of irregularities due to the placement of contaminant ions on the adsorption sites (Samadani, 2013; Samadani et al., 2015).

Fig. 4 shows the absorption capability of CNF aerogel to remove nitrate, nitrite and phosphate compounds during successive three cyclic absorption/desorption process. The result showed that the maximum absorption of nitrate, nitrite and phosphate, was respectively 77.09%, 67.82%, 81.81%, happened in the first cycle, while the corresponding minimum absoption values (65.47%, 49.56%, 60% respectively) occurred at third cycle.

Table 2 are present isothermal equations for the adsorption of nitrogen and phosphate compounds. The Langmuir model is based on the assumption of monolayer and homogeneous adsorption with the same energy. The Freundlich model is based on multilayer adsorption with heterogeneous surfaces and heterogeneous distribution of energy, and the Temkin isotherm model indicates the decrease in absorption heat of all molecules at the adsorbent surface. The equilibrium adsorption data indicate that they have the highest compliance with the Temkin isotherm model than the Langmuir and Freundlich models with a correlation coefficient of 0.93 for nitrate, 0.99 for nitrite and 0.86 for phosphate. After that, the highest compliance of phosphate is related to the Langmuir model with a coefficient of 0.84 and nitrate with Freundlich and Langmuir models with coefficients of 0.82 and 0.73 and nitrite with coefficients of 0.96 and 0.92, respectively. In the Freundlich model, high Kf indicates high adsorption capacity. The highest amount of 254.67 mg was observed in the nitrite. The larger or smaller q_{max} in the Langmuir model represents the abundance of adsorption sites per unit mass of adsorbent and causes a large number of ions to be adsorbed at the nano-adsorbent surface. Study of first pseudo and second-order kinetic equations shows more compliance with the second pseudo model with coefficients of 0.99, 0.98 and 0.99 for nitrate, nitrite and phosphate, respectively. The kinetics is used to evaluate the speed of the adsorption process.

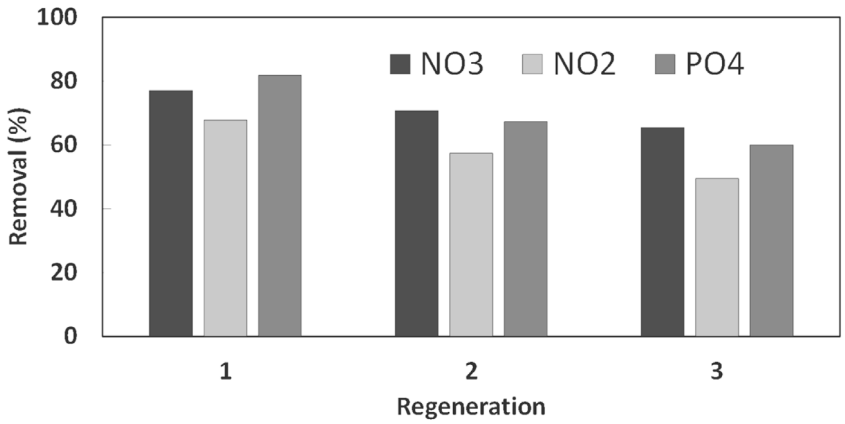

Fig. 4. Absorption capability of CNF aerogel to remove nitrate, nitrite and phosphate compounds during successive three cyclic absorption/desorption process.

Table 2
Isotherm (a) and kinetic models (b) coefficients for waste water parameters (NO3, NO2, PO4).

(a) Isotherm models

	Langmuir			Freundlich			Temkin		
	K_L (l/mg^{-1})	q_m^{exp} (mg/g^{-1})	R^2	K_f (l/mg^{-1})	N	R^2	K_T (l/mg^{-1})	B_T	R_2
NO3	0/85	4/58	0/73	15/33	4/78	0/82	1/82	12/82	0/93
NO2	4/34	0/88	0/92	254/67	4/20	0/96	2/29	1/87	0/99
PO4	83/33	1/08	0/84	10/48	1/58	0/73	7/46	0/60	0/86

(b) Kinetic models

	Pseudo first order			Pseudo second order		
	K_1 (min^{-1})	qe (mg/g^{-1})	R^2	qe (mg/g^{-1})	K_2 (min^{-1})	R^2
NO3	0/01	2/48	0/29	4/76	0.12	0/99
NO2	0/016	22/10	0/35	0/89	0/28	0/98
PO4	0/0163	3	0/36	1/07	17/54	0/99

The second-order kinetics represents the chemical adsorption and the deceleration rate and the adsorption controller, where the compliance of the ions with the second-order kinetics represent the chemical adsorption.

Table 3 the thermodynamic parameters. Some of the reactions are natural and some of them are done with the help of external factors. Thermodynamics studies deal with the reversible and irreversible chemical reactions. By increasing the temperature, the Gibbs free energy will decrease, which represents a spontaneous reaction. Negative enthalpy and entropy indicate the spontaneity of a reaction at low temperature which represents the reversibility of the reaction and the equilibrium of the reaction. The negative enthalpy indicates the exothermic reaction. Gibbs free energy values of less than −20 kJ/mol represent physical adsorption. According to Le Chatelier's Principle, the maximum adsorption capacity decreases with increasing temperature.

The evaluation of adsorption isotherm models represents the affinity of adsorbent and surface properties, which can be changed depending on the type of adsorbent (Hafshejani et al., 2016). Investigating the parameters of adsorption capacity and intensity in nitrate, nitrite and phosphate compounds revealed high adsorption capacity in nitrite with 254.67 l/mg and phosphate with 83.33 l/mg and nitrate with 15.33 in l/mg. According to KL coefficient, maximum adsorption energy is related to the adsorption of phosphate. The greater the Kf, the greater the adsorption capacity of the adsorbent . In this regard, the highest rate is observed in the nitrite, indicating very high capacity of adsorbent for the adsorption of nitrite ions. In the Freundlich equation, the coefficient n is the empirical parameter related to the stability of the adsorbent. This coefficient should be less than 10 and greater than 1 for an optimal adsorption process, which was calculated to be 4.78, 4.20 and 1.58 in the nitrate, nitrite and phosphate ions, respectively. The highest matching of RL is related to the Temkin and Langmuir models that the most suitable mode for the adsorption of nitrite with 0.99, phosphate with 0.86 and nitrate with 0.93 was respectively observed. The value of RL less than 1 represents the suitability of the isotherm and the adsorption process. The matching of the adsorption models with the Temkin model can be due to the heterogeneous distribution of the adsorption sites and the adsorbate–adsorbent interaction. Evaluation of the effect of contact time on adsorption rate and adsorbent capacity, which is proposed as kinetics also indicates the equilibrium time and reaction pathway (Samadani et al., 2015), which indicates a greater matching with the second pseudo order model with adsorption coefficients of 0.99, 0.98 and 0.99 for nitrate, nitrite and phosphate, respectively. In a study conducted by Rafieian et al. (2018), they employed hydrophobic coatings using the chemical vapor of hexadecyltrimethoxylan in the nano-cellulose

Table 3
Thermodynamic parameters at different temperatures (PO4, NO2, NO3).

T (K)	ΔG° (kj/mol)	ΔH° (kj/mol)	ΔS° (kj/mol K^{-1})
298	−9/38	−63/02	−0/18
303	−8/48	*	*
313	−6/68	*	*
323	−4/88	*	*
T (K) (NO2)	ΔG° (kj/mol)	ΔH° (kj/mol)	ΔS° (kj/mol K^{-1})
298	−6/43	−71/99	−0/22
303	−5/33	*	*
313	−3/13	*	*
323	−0/93	*	*
T (K) (NO3)	ΔG° (kj/mol)	ΔH° (kj/mol)	ΔS° (kj/mol K^{-1})
298	−3/69	−39/45	−0/12
303	−3/09	*	*
313	−1/89	*	*
323	−0/69	*	*

aerogel structure that caused the produced aerogels to have features such as a density of 11–17.5 mg/cm^3 and a porosity of equal to 99.3% and 98.8%, respectively (Rafieian et al., 2018). The aerogel produced in this study had a porosity of 99.68% and a specific surface area of 300 m^2/g, and a density of 0.004 g/cm^3, which represents the high capability of aerogels generated with fully biological compounds without the use of chemical compounds. In another study carried out by Hoon Kim et al. (2015), on examining the effect of using maleic acid and sodium hypophosphite as connectors on cellulose nanofiber aerogels, these connectors showed the ability of the aerogel to remain in the water for 1 min (Kim et al., 2015), while the aerogels produced in this study, by creating strong crosslinks between CA and CMC with cellulose nanofibril hydroxyl groups, were able to stay in water for more than 90 min. Finally, all of examined parameters resulted in the design of a wastewater treatment system model with nano-cellulose aerogels, which is schematically shown in Fig. 5.

In design of the effluent design system for fish farms, effluent discharged into the sediment storage tanks first passes through the filters equipped with mesh filters to allow the untreated material to pass through the filters. The effluent then enters the tanks equipped with rotary reactors and propulsion turbines that are constantly monitored for acidity and temperature. The effluent is then discharged into the first and second sediment storage tanks to then remove soluble and suspended solids and then into rotor-equipped reactors to hydrogen-purify the tanks and rotate the turbines equipped with nano-cellulose aerogels to purify nitrogen compounds and phosphate, finally the treated effluent enters the collection tanks (Fig. 5). In the batch reactor system, the combustors are initially introduced into the reactor and are strongly mixed for a specified period of time and then discharged after the specified time has elapsed and the reaction progresses. No mass enters or exits during the reactor operation. Temperature control in the reactors is important because of the heat and the warming of the reactions. As a result, the contents inside the reactor may become hot and cold during operation and may disrupt the reaction and equipment. Heat exchangers are used to adjust the temperature. Pipes with hot and cold flow around the reactors can be used. Stir operation in reactors is important because if the mixing and transfer speeds are not well established, there is no possibility of a reaction between the adsorbent and the adsorbent material. The mixer shape design depends on the volume and shape of the tank and the intensity of the flow. The use of polymer reactors makes the temperature throughout the reactor uniform.

4. Conclusions

In this study, the use of novel aerogel with biological structures without any harmful chemical compounds at low cost with high water adsorption capacity and shape memory capability could be well applied in water and wastewater treatment processes. The results revealed that the produced CNF aerogels had a high specific surface area and high porosity and low density and, following the Temkin and Langmuir adsorption models and the second pseudo kinetics model, can act as an suitable adsorbent for reduction and remove of nitrite, nitrate and phosphate compounds by 79.65, 73.04 and 98.18 mg/l. According to the standard of water input for farmlands, the allowed amount of compounds should be for nitrate (less than 2 mg per liter), nitrite (less than 0.1 mg per liter) and phosphate (between 0.2 and 0.5 mg per liter), these allowed amounts of compounds could be achieved using the CNF aerogel as nano-adsorbent.

Declaration of competing interest

The authors declare that they have no known competing financial interests or personal relationships that could have appeared to influence the work reported in this paper.

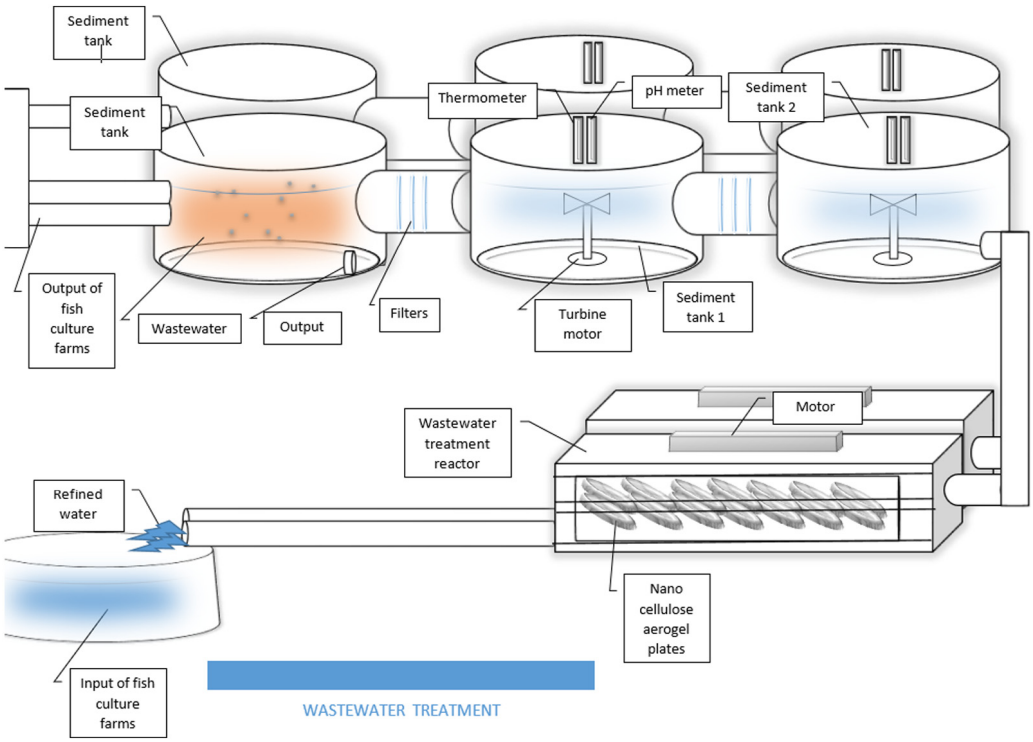

Fig. 5. Modeling of wastewater treatment system produced with nano cellulose aerogels.

CRediT authorship contribution statement

Fatemeh Darabitabar: Methodology, Writing - original draft, Visualization. **Vahid Yavari:** Conceptualization, Supervision, Validation. **Aliakbar Hedayati:** Funding acquisition, Project administration, Resources, Writing - review & editing. **Mohammad Zakeri:** Validation, Investigation, Data curation. **Hossein Yousefi:** Software, Data curation, Formal analysis.

Funding

This research was financially supported by the Iran National Science Foundation (INSF) [grant number 96017217].

References

Askari Hesni, Majid, Hedayati, Aliakbar, Qadermarzi, Amir, Pouladi, Mojtaba, Zangiabadi, Somayeh, Naqshbandi, Nabat, 2020. Using chlorella vulgaris and iron oxide nanoparticles in a designed bioreactor for aquaculture effluents purification. Aquac. Eng. 90 (4), 102069. http://dx.doi.org/10.1016/j.aquaeng.2020.102069.

Azadbakht, P., Pourzamani, H., Petroudy, S.R.J., Bina, B., 2016. Removal of nitrate from aqueous solution using nanocrystalline cellulose. Int. J. Environ. Health Eng. 5 (1), 17.

Ciolacu, D., Ciolacu, F., Popa, V.I., 2011. Amorphous cellulose—structure and characterization. Cellulose Chem. Technol. 45 (1), 13.

Coma, V., Sebti, I., Pardon, P., Pichavant, F., Deschamps, A., 2003. Film properties from crosslinking of cellulosic derivatives with a polyfunctional carboxylic acid. Carbohydr. Polymers 51 (3), 265–271.

Dashipour, A., Khaksar, R., Hosseini, H., Shojaee-Aliabadi, S., Kiandokht, G., 2014. Physical, antioxidant and antimicrobial characteristics of carboxymethyl cellulose edible film cooperated with clove essential oil. Zahedan J. Res. Med. Sci. 16 (8), 34–42.

De France, K.J., Hoare, T., Cranston, E.D., 2017. Review of hydrogels and aerogels containing nanocellulose. Chem. Mater. 29 (11), 4609–4631.

Demitri, C., Del Sole, R., Scalera, F., Sannino, A., Vasapollo, G., Maffezzoli, A., et al., 2008. Novel superabsorbent cellulose-based hydrogels crosslinked with citric acid. J. Appl. Polym. Sci. 110 (4), 2453–2460.

Ebrahimi, M., Langeroodi, N.S., Hooshmand, S., 2019. Biosorption of Fe (III) ions using Carrot: Equilibrium, kinetics, and statistical analysis. Prot. Met. Phys. Chem. Surf. 55 (2), 259–265.

Fan, M., Dai, D., Huang, B., 2012. Fourier transform infrared spectroscopy for natural fibres. In: Fourier Transform-Materials Analysis. Intechopen.

Gopakumar, D.A., Pottathara, Y.B., Sabu, K., Khalil, H.A., Grohens, Y., Thomas, S., 2019. Nanocellulose-based aerogels for industrial applications. In: Industrial Applications of Nanomaterials. Elsevier, pp. 403–421.

Haafiz, M.M., Eichhorn, S., Hassan, A., Jawaid, M., 2013. Isolation and characterization of microcrystalline cellulose from oil palm biomass residue. Carbohydr. Polymers 93 (2), 628–634.

Hafshejani, L.D., Hooshmand, A., Naseri, A.A., Mohammadi, A.S., Abbasi, F., Bhatnagar, A., 2016. Removal of nitrate from aqueous solution by modified sugarcane bagasse biochar. Ecol. Eng. 95, 101–111.
Jana, B.B., Mandal, R.N., Jayasankar, D.P., 2018. Wastewater Management Through Aquaculture (Vol. 1). Springer Singapore.
Kaya, M., 2017. Super absorbent, light, and highly flame retardant cellulose-based aerogel crosslinked with citric acid. J. Appl. Polym. Sci. 134 (38), 45315.
Kim, C.H., Youn, H.J., Lee, H.L., 2015. Preparation of cross-linked cellulose nanofibril aerogel with water absorbency and shape recovery. Cellulose 22 (6), 3715–3724.
Langeroodi, N.S., 2017. Equilibrium and kinetics of biosorption of oxalic acid by wheat straw. Russ. J. Phys. Chem. B 11 (2), 318–323.
Long, L.-Y., Weng, Y.-X., Wang, Y.-Z., 2018. Cellulose aerogels: Synthesis, applications, and prospects. Polymers 10 (6), 623.
LoPachin, R.M., 2004. The changing view of acrylamide neurotoxicity. Neurotoxicology 25 (4), 617–630.
Morán, J.I., Alvarez, V.A., Cyras, V.P., Vázquez, A., 2008. Extraction of cellulose and preparation of nanocellulose from sisal fibers. Cellulose 15 (1), 149–159.
Ogushi, Y., Sakai, S., Kawakami, K., 2007. Synthesis of enzymatically-gellable carboxymethylcellulose for biomedical applications. J. Biosci. Bioeng. 104 (1), 30–33.
Rafieian, F., Hosseini, M., Jonoobi, M., Yu, Q., 2018. Development of hydrophobic nanocellulose-based aerogel via chemical vapor deposition for oil separation for water treatment. Cellulose 25 (8), 4695–4710.
Reddy, N., Yang, Y., 2005. Structure and properties of high quality natural cellulose fibers from cornstalks. Polymer 46 (15), 5494–5500.
Reddy, N., Yang, Y., 2010. Citric acid cross-linking of starch films. Food Chem. 118 (3), 702–711.
Safaei, E., Langeroodi, N.S., Baher, E., 2019. Investigation of removal of Cu (II) ions by commercial activated carbon: Equilibrium and thermodynamic studies. Prot. Met. Phys. Chem. Surf. 55 (1), 28–33.
Samadani, N., 2013. Study of the adsorption of acetic acid on silica gel in aqueous solution. Rev. Roum. Chim. 58 (1), 43–48.
Samadani, N., Taheri, F., Mehrani, S., 2015. Thermodynamic and kinetic investigation of citric acid adsorption by rice bran. Nova Biol. Repert. 2 (3), 166–175.
Sehaqui, H., Zhou, Q., Berglund, L.A., 2011. High-porosity aerogels of high specific surface area prepared from nanofibrillated cellulose (NFC). Compos. Sci. Technol. 71 (13), 1593–1599.
Shamskar, K.R., Heidari, H., Rashidi, A., 2019. Study on nanocellulose properties processed using different methods and their aerogels. J. Polym. Environ. 27 (7), 1418–1428.
Shi, R., Zhang, Z., Liu, Q., Han, Y., Zhang, L., Chen, D., Tian, W., 2007. Characterization of citric acid/glycerol co-plasticized thermoplastic starch prepared by melt blending. Carbohydr. Polymers 69 (4), 748–755.
Tajari, E., Langeroodi, N.S., Khalafi, M., 2019. Statistical modeling, optimization and kinetics of Mn2+ adsorption in aqueous solution using a biosorbent. Z. Phys. Chem. 233 (8), 1201–1214.
Tian, C., She, J., Wu, Y., Luo, S., Wu, Q., Qing, Y., 2018. Reusable and cross-linked cellulose nanofibrils aerogel for the removal of heavy metal ions. Polym. Compos. 39 (12), 4442–4451.
Wei, J., Yang, Z., Sun, Y., Wang, C., Fan, J., Kang, G., Li, Y., 2019. Nanocellulose-based magnetic hybrid aerogel for adsorption of heavy metal ions from water. J. Mater. Sci. 54 (8), 6709–6718.
Yousefi, H., Azad, S., Mashkour, M., Khazaeian, A., 2018. Cellulose nanofiber board. Carbohydr. Polymers 187, 133–139.
Yousefi, H., Mashkour, M., Yousefi, R., 2015. Direct solvent nanowelding of cellulose fibers to make all-cellulose nanocomposite. Cellulose 22 (2), 1189–1200.
Zheng, Q., Cai, Z., Gong, S., 2014. Green synthesis of polyvinyl alcohol (PVA)–cellulose nanofibril (CNF) hybrid aerogels and their use as superabsorbents. J. Mater. Sci. A 2 (9), 3110–3118.
Zheng, W.J., Gao, J., Wei, Z., Zhou, J., Chen, Y.M., 2015. Facile fabrication of self-healing carboxymethyl cellulose hydrogels. Eur. Polym. J. 72, 514–522.